Cell Reports, Volume *42*

Supplemental information

Sequential activation of E2F via Rb degradation and c-Myc drives resistance to CDK4/6 inhibitors in breast cancer

Sungsoo Kim, Jessica Armand, Anton Safonov, Mimi Zhang, Rajesh K. Soni, Gary Schwartz, Julia E. McGuinness, Hanina Hibshoosh, Pedram Razavi, Minah Kim, Sarat Chandarlapaty, and Hee Won Yang

SUPPLEMENTARY ITEMS

Figure S1: Subsets of breast cancer cells expressing intact Rb adapt to CDK4/6i following initial response. Related to Figure 1.

Figure S2: Subsets of breast cancer cells adapt to CDK4/6i regardless of Rb expression levels. Related to Figure 1.

Figure S3: Expression levels of Rb protein are reduced in CDK4/6i-resistant cells relative to drug-naïve cells. Related to Figure 2.

Figure S4: Targeting proteasome activity prevents Rb-protein reduction mediated by CDK4/6i treatment. Related to Figure 3.

Figure S5: Treatment with proteasome inhibitors restores Rb-protein levels and suppress the growth of CDK4/6i-resistant cells. Related to Figure 3.

Figure S6: CDK4/6i treatment increases heterogeneity in E2F and CDK2 activation kinetics. Related to Figure 4.

Figure S7: Breast cancer cells entering quiescence reduce Rb-protein levels in both persister and non-persister cells. Related to Figure 5.

Figure S8: Rb knockout alone is sufficient to induce CDK4/6i adaptation. Related to Figure 6.

Figure S9: Targeting mitogenic or endocrine signaling inhibits c-Myc, global transcription rate, and CDK4/6i resistance. Related to Figure 6.

Figure S10: c-Myc amplifies E2F activity to facilitate the development of CDK4/6i-tolerant persisters following Rb-protein reduction. Related to Figure 7.

Figure S11: Lack of correlation between Rb levels and PFS in pre-treatment FFPE tumor samples. Related to Figure 7.

Table S1: Primers for Real-Time PCR. Related to STAR Methods.

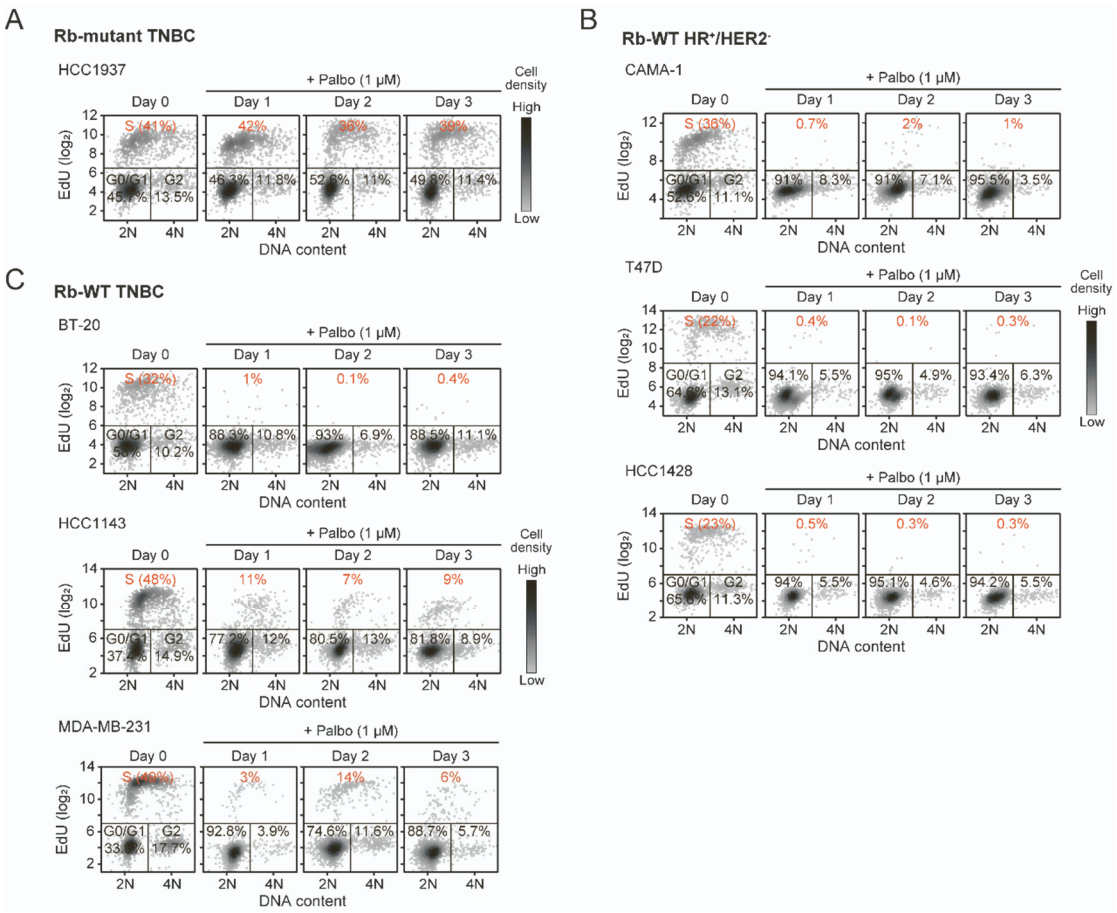

Figure S1. Subsets of breast cancer cells expressing intact Rb adapt to CDK4/6i following initial response. Related to Figure 1.

(**A**–**C**) Density scatterplots of Hoechst and EdU staining in *Rb*-mutant TNBC (A) and Rb-WT $HR^+/HER2^-$ breast cancer (B) and TNBC (C) cells treated with palbociclib (1 μM) for the indicated durations (n = 2,000 cells/condition).

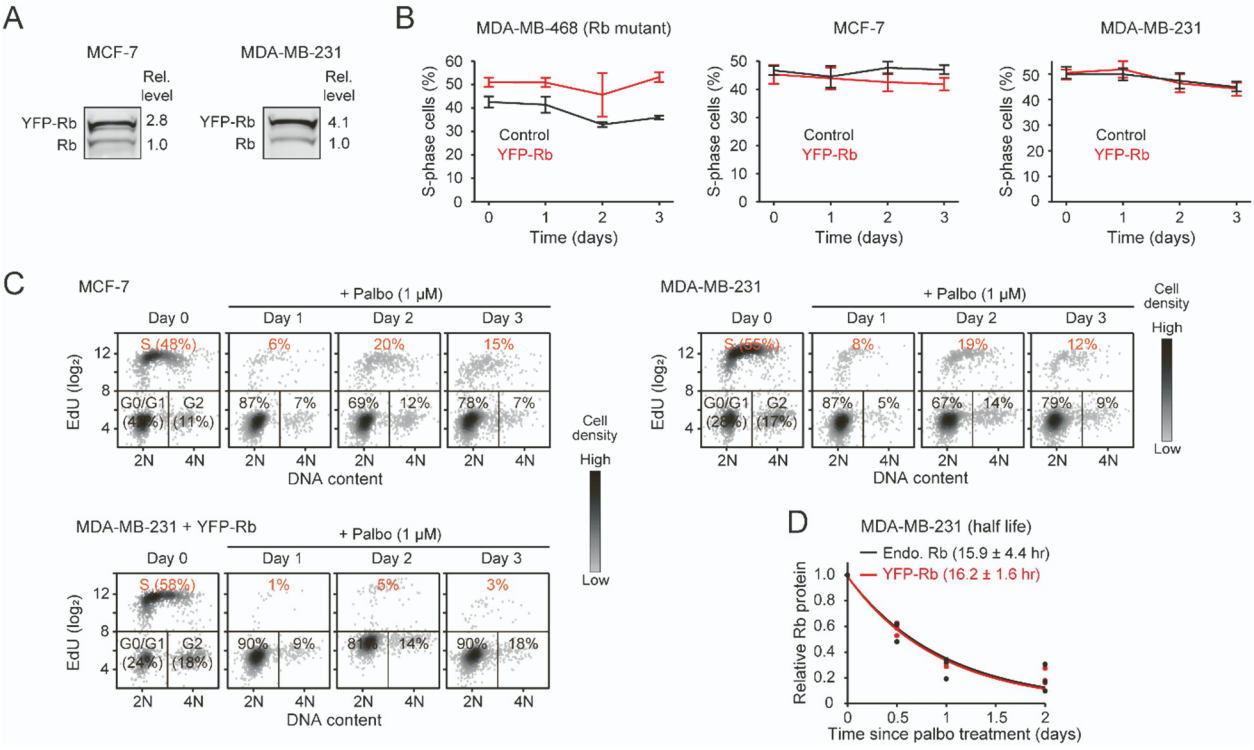

Figure S2. Subsets of breast cancer cells adapt to CDK4/6i regardless of Rb expression levels. Related to Figure 1.

(**A**) Immunoblot showing endogenous Rb and exogenous YFP-Rb protein expression in MCF-7 and MDA-MB-231 cells. Numbers represent relative YFP-Rb levels normalized to endogenous Rb levels.

(**B**) Percentage of S-phase cells in *Rb*-mutant MDA-MB-468, MCF-7, and MDA-MB-231 cells with or without YFP-Rb overexpression. Data are shown as means ± SD (n = 3 biological replicates).

(**C**) Density scatterplots of Hoechst and EdU in MCF-7 without YFP-Rb expression and MDA-MB-231 cells without or with YFP-Rb expression. Cells were treated with palbociclib (1 μM) for the indicated durations (n = 2,000 cells/condition).

(**D**) Relative levels of endogenous and exogenous Rb protein in MDA-MB-231 cells treated with palbociclib (1 μM) for the indicate durations (0–2 days). Solid lines indicate best fitted lines. The half-life of Rb protein are indicated. Data are shown as means ± SD (n = 3 biological replicates).

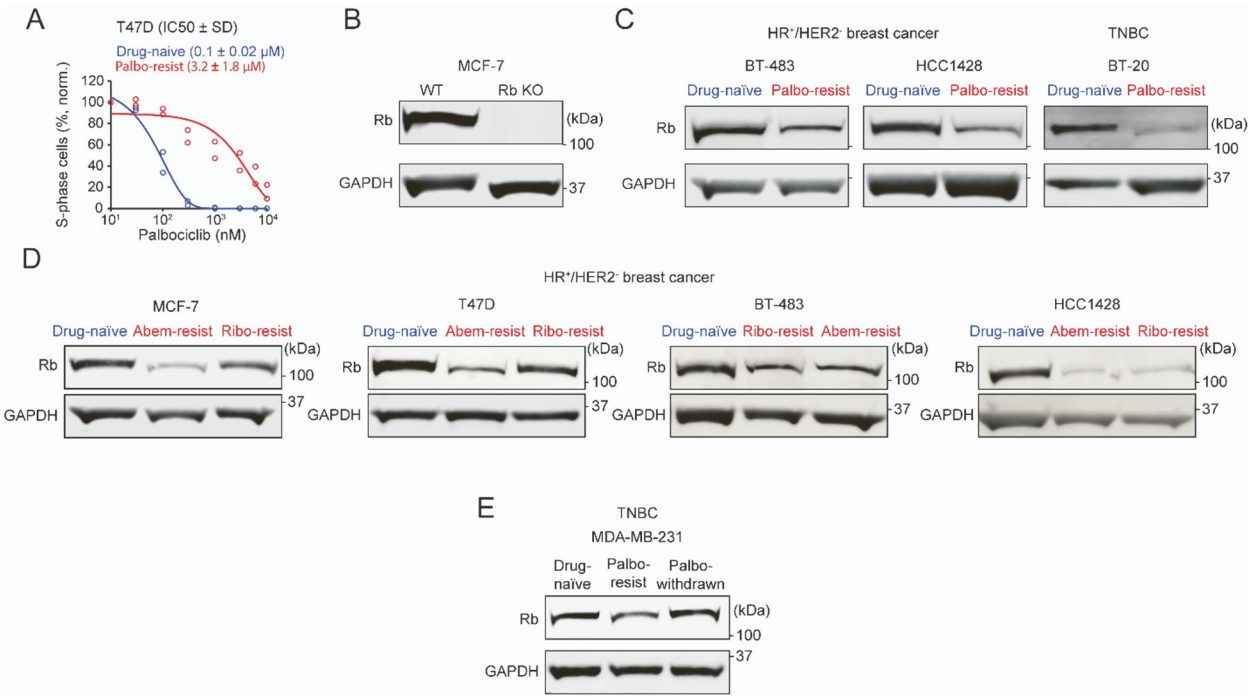

Figure S3. Expression levels of Rb protein are reduced in CDK4/6i-resistant cells relative to drug-naïve cells. Related to Figure 2.

(**A**) Dose-response curves for palbociclib treatment (48 hr) in drug-naïve and palbociclib-resistant T47D cells. IC50 values are shown as means ± SD (n = 2 biological replicates).

(**B**) Immunoblot showing Rb and GAPDH expression in wild-type and Rb-knockout MCF-7 cells.

(**C**) Immunoblot showing Rb, and GAPDH expression in drug-naïve and palbociclib-resistant BT-483, HCC1428, and BT-20 cells.

(**D**) Immunoblot showing Rb and GAPDH expression in drug-naïve, ribociclib (1 μM)-resistant, abemaciclib (1 μM)-resistant MCF-7, T47D, BT-483, and HCC1428 cells.

(**E**) Immunoblot showing Rb and GAPDH expression in drug-naïve, palbociclib-resistant MDA-MB-231 cells with continued palbociclib (1 μM) treatment and after withdrawal for over 1 week.

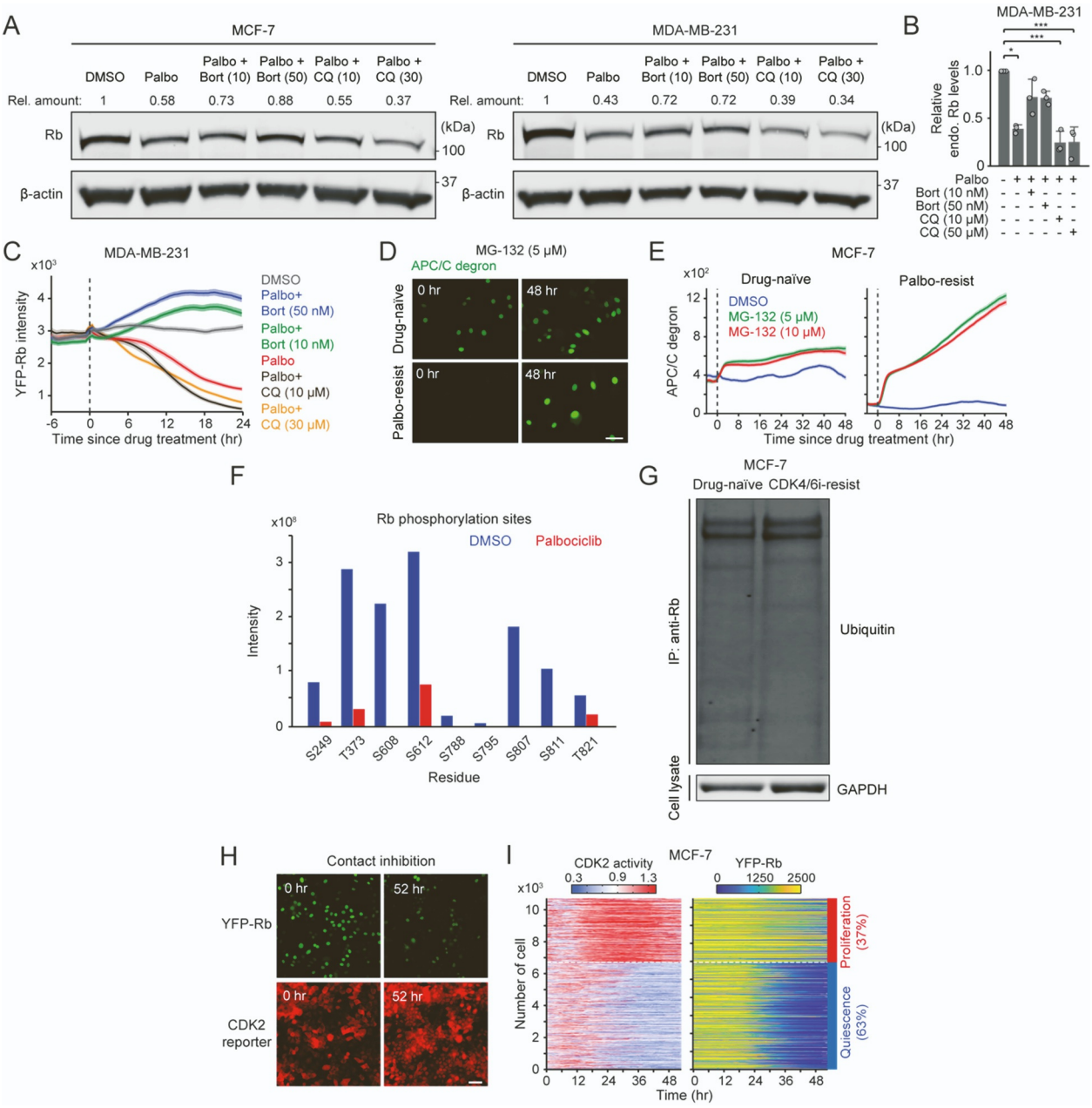

Figure S4. Targeting proteasome activity prevents Rb-protein reduction mediated by CDK4/6i treatment. Related to Figure 3.

(**A**) Immunoblot showing Rb and GAPDH expression in drug-naïve MCF-7 and MDA-MB-231 cells treated with combinations of palbociclib (1 μM), bortezomib (10 or 50 nM), and chloroquine (10 or 30 μM) for 24 hr.

(**B**) Relative endogenous Rb levels in MDA-MB-231 cells after treating with indicated drugs. Data are means ± SD (n = 3 biological replicates). Data are means ± SD (n = 3 biological replicates). P values were calculated by one-way ANOVA (* $p \leq 0.05$; *** $p \leq 0.0001$).

(C) Average traces of YFP-Rb intensities in MDA-MB-231 cells. Data are shown as means ± 95% CI (DMSO, n = 1,069 cells; palbo, n = 1,365 cells; palbo + bort (10), n = 1,421 cells; palbo + bort (50), n = 1,622 cells; palbo + CQ (10), n = 961 cells; palbo + CQ (30), n = 1,696 cells).

(**D**) Representative images of APC/C degron in drug-naïve and palbociclib-resistant MCF-7 cells before and after 48 hr treatment with MG-132 (5 μM). Scale bar is 100 μm.
(**E**) Averaged traces of APC/C degron levels in drug-naïve and palbociclib-resistant MCF-7 cells after DMSO and MG-132 (5 μM or 10 μM) treatment. Data are means ± 95% CI (DMSO, n = 8,814 cells; 5 μM MG-132, n = 4,425 cells; 10 μM MG-132, n = 6,357 cells).
(**F**) Changes in Rb phosphorylation sites detected by mass-spectrometry analysis after treatment with DMSO or palbociclib (1 μM) + bortezomib (50 nM) for 24 hr.
(**G**) Immunoblot showing ubiquitination after immunoprecipitation of Rb in drug-naïve and palbociclib-resistant MCF-7 cells. Cells were treated MG-132 (5 μM) for 1 hr before collecting lysates.
(**H**) Representative images of YFP-Rb and CDK2 reporter before and after contact inhibition. Scale bar is 100 μm.
(**I**) Heatmaps of single-cell traces for CDK2 activity and YFP-Rb intensity in MCF-7 cells. Each row represents a single-cell trace. Percentages indicate the proportion of proliferation (CDK2 activity > 1.0 for over 2 hr) and quiescence (no CDK2 activation) cells, based on CDK2 activity 36–52 hr post-treatment.

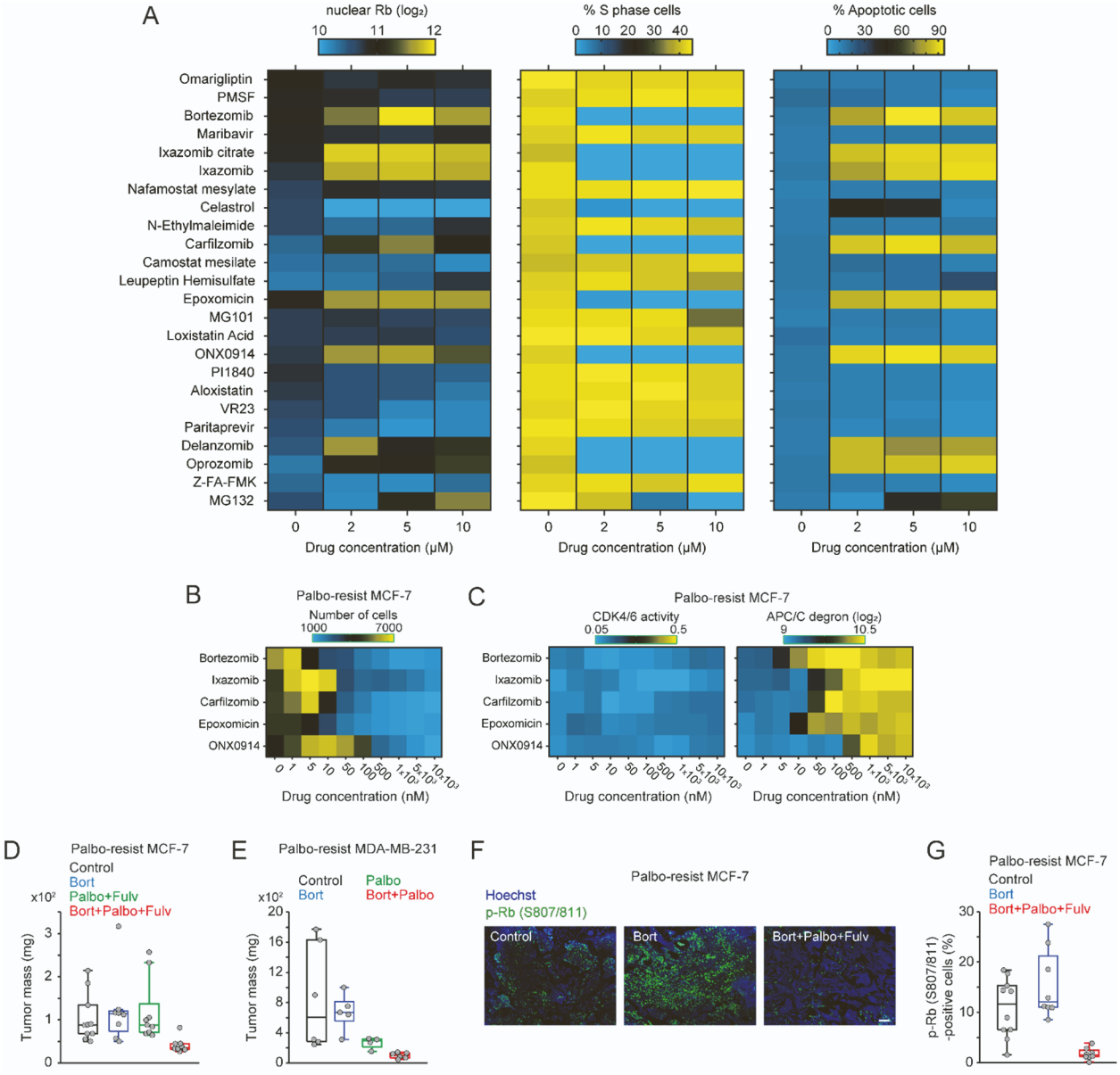

Figure S5. Treatment with proteasome inhibitors restores Rb-protein levels and suppress the growth of CDK4/6i-resistant cells. Related to Figure 3.

(**A**) Heatmaps of nuclear Rb levels, percentage of S-phase, and apoptotic cells according to the color map. Palbociclib-resistant MCF-7 cells were treated with indicated proteasome inhibitors (0, 2, 5, and 10 μM) in the presence of palbociclib (1 μM) for 48 hr (n > 1,000 cells/condition).

(**B** and **C**) Heatmap of the number of cells (B), endogenous CDK4/6 activity, and APC/C degron intensity (C) according to the color map. Palbociclib-resistant MCF-7 cells were treated with indicated proteasome inhibitors (0–10 μM) in the presence of palbociclib (1 μM) for 48 hr (n > 1,000 cells/condition).

(**D** and **E**) Box plot of tumor mass in MCF-7 (D) and MDA-MB-231 (E) xenografts. Middle lines indicate the median, boxes represent the 25th and 75th percentiles, and lines denote the total range for each population (D: control, n = 10 mice; bort, n = 8 mice; palbo + fulv, n = 9 mice; bort +

palbo + fulv, *n* = 8 mice; E: control, *n* = 6 mice; bort, *n* = 5 mice; palbo, *n* = 4 mice; bort + palbo, *n* = 6 mice).
(**F**) Representative images of Hoechst and phosphorylated Rb (p-Rb) at S807/811 staining in tumor tissues. Scale bar is 100 μm.
(**G**) Box plot of the percentage of p-Rb-positive cells (control, *n* = 10 mice; bort, *n* = 8 mice; bort + palbo + fulv, *n* = 8 mice).

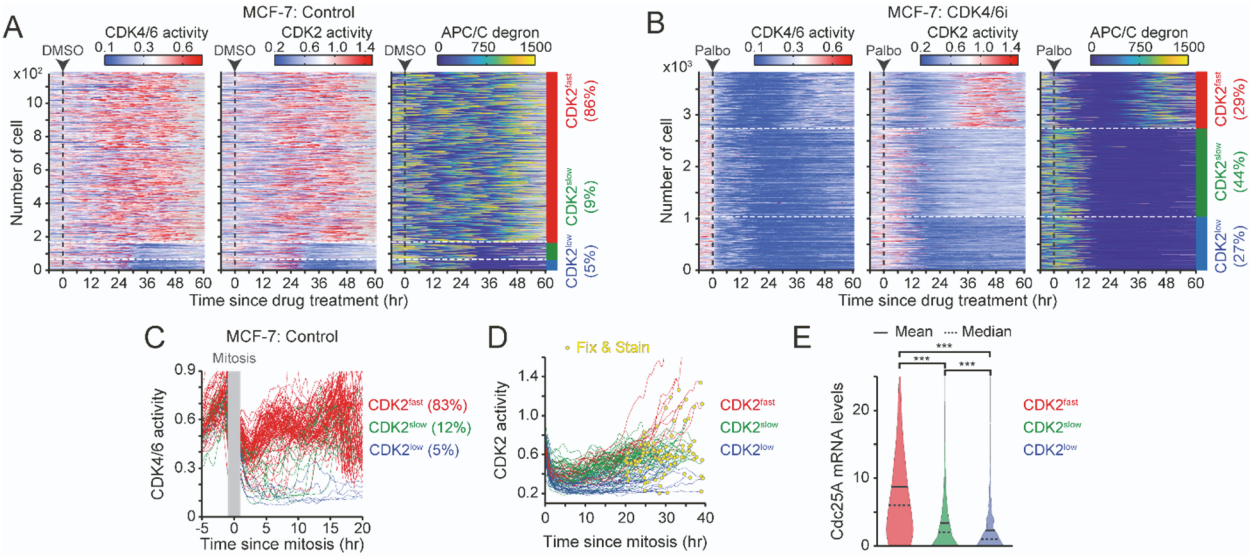

Figure S6. CDK4/6i treatment increases heterogeneity in E2F and CDK2 activation kinetics. Related to Figure 4.

(**A** and **B**) Heatmaps of single-cell traces for CDK4/6 and CDK2 activities and APC/C degron intensity in MCF-7 cells treated with either DMSO (A) or palbociclib (1 μM) (B). Each row represents a single-cell trace. Percentages indicate the proportion of $CDK2^{fast}$ (CDK2 activity > 1.0 for over 2 hr), $CDK2^{slow}$ (CDK2 activity > 0.6 for over 2 hr), and $CDK2^{low}$ (no CDK2 activation) cells, based on CDK2 activity 30–60 hr post-treatment. Arrow and black dotted line mark the drug-treatment time.

(**C**) Single-cell traces for CDK4/6 activity aligned by mitosis in MCF-7 cells treated with DMSO.

(**D**) Single-cell traces for CDK2 activity aligned to the time after mitosis. MCF-7 cells were treated with palbociclib (1 μM) and classified based on CDK2 activity as described in (A and B). Yellow points correspond to the time of fixation.

(**E**) Cdc25A mRNA level in MCF-7 cells classified based on CDK2 activation kinetics after palbociclib (1 μM) treatment ($CDK2^{fast}$, n = 1,098 cells; $CDK2^{slow}$, n = 5,584 cells; $CDK2^{low}$, n = 2,566 cells). P values were calculated by one-way ANOVA (*** $p \leq 0.0001$).

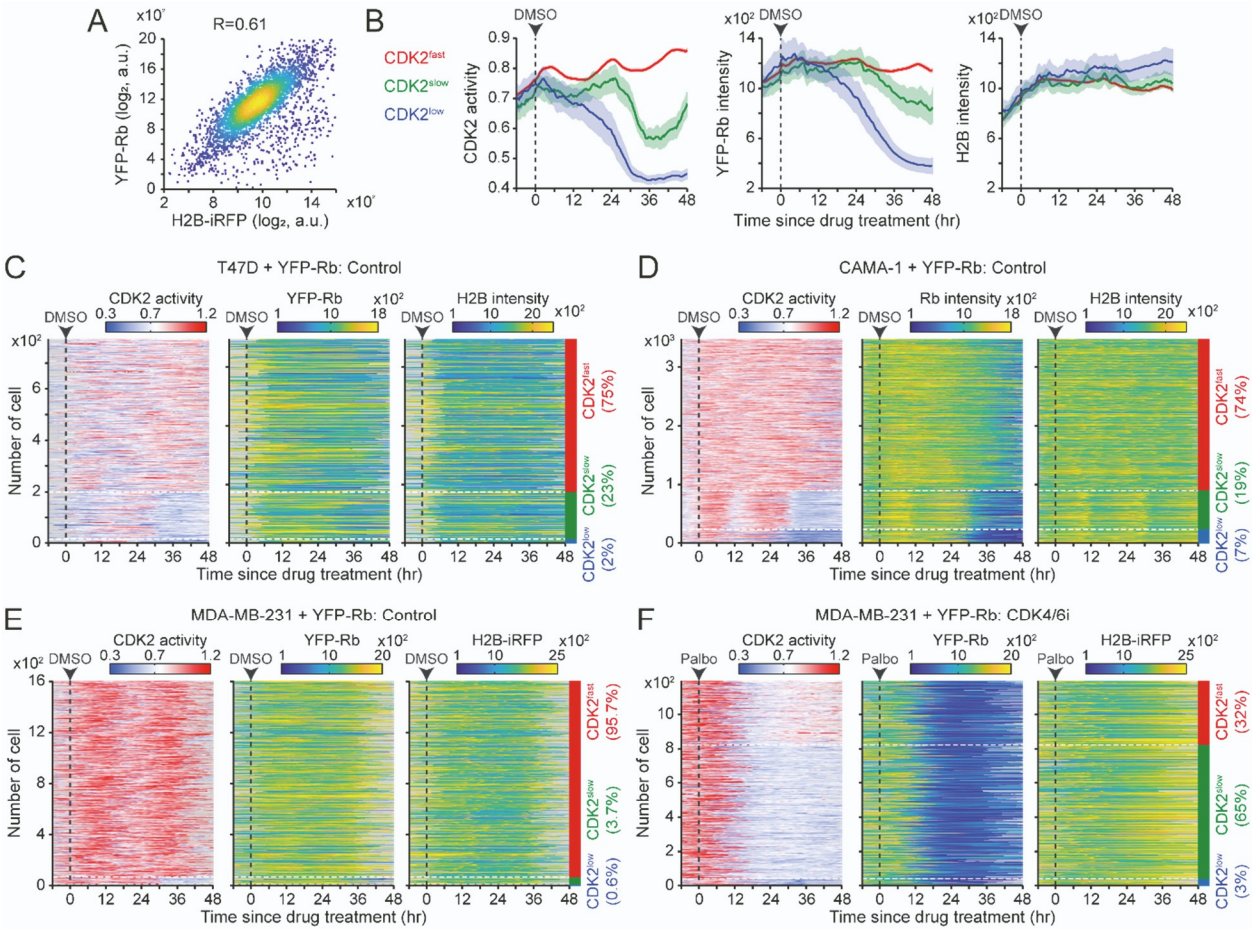

Figure S7. Breast cancer cells entering quiescence reduce Rb-protein levels in both persister and non-persister cells. Related to Figure 5.

(**A**) Density scatterplot of YFP-Rb versus H2B-iRFP intensity in Rb-knockout MCF-7 cells expressing the YFP-Rb–p2a–H2B-iRFP construct. The correlation value (R) between YFP-Rb and H2B-iRFP intensities is indicated.

(**B**) Average traces of CDK2 activity and YFP-Rb and H2B-iRFP intensities in Rb-knockout MCF-7 cells expressing YFP-Rb treated with DMSO ($CDK2^{fast}$, n = 4,314 cells; $CDK2^{slow}$, n = 68 cells; $CDK2^{low}$, n = 64).

(**C**–**F**) Heatmaps of single-cell traces for CDK2 activity and YFP-Rb and H2B-iRFP intensities in T47D (C) and CAMA-1 (D) cells treated with DMSO and MDA-MB-231 cells treated with DMSO (E) or palbociclib (1 μM) (F). Each row represents a single-cell trace. The percentages denote the proportion of $CDK2^{fast}$ (CDK2 activity > 0.8 for over 2 hr), $CDK2^{slow}$ (CDK2 activity > 0.6 for over 2 hr), and $CDK2^{low}$ (no CDK2 activation) cells, classified based on CDK2 activity 30–48 hr post-treatment. Arrow and black dotted line mark the drug-treatment time.

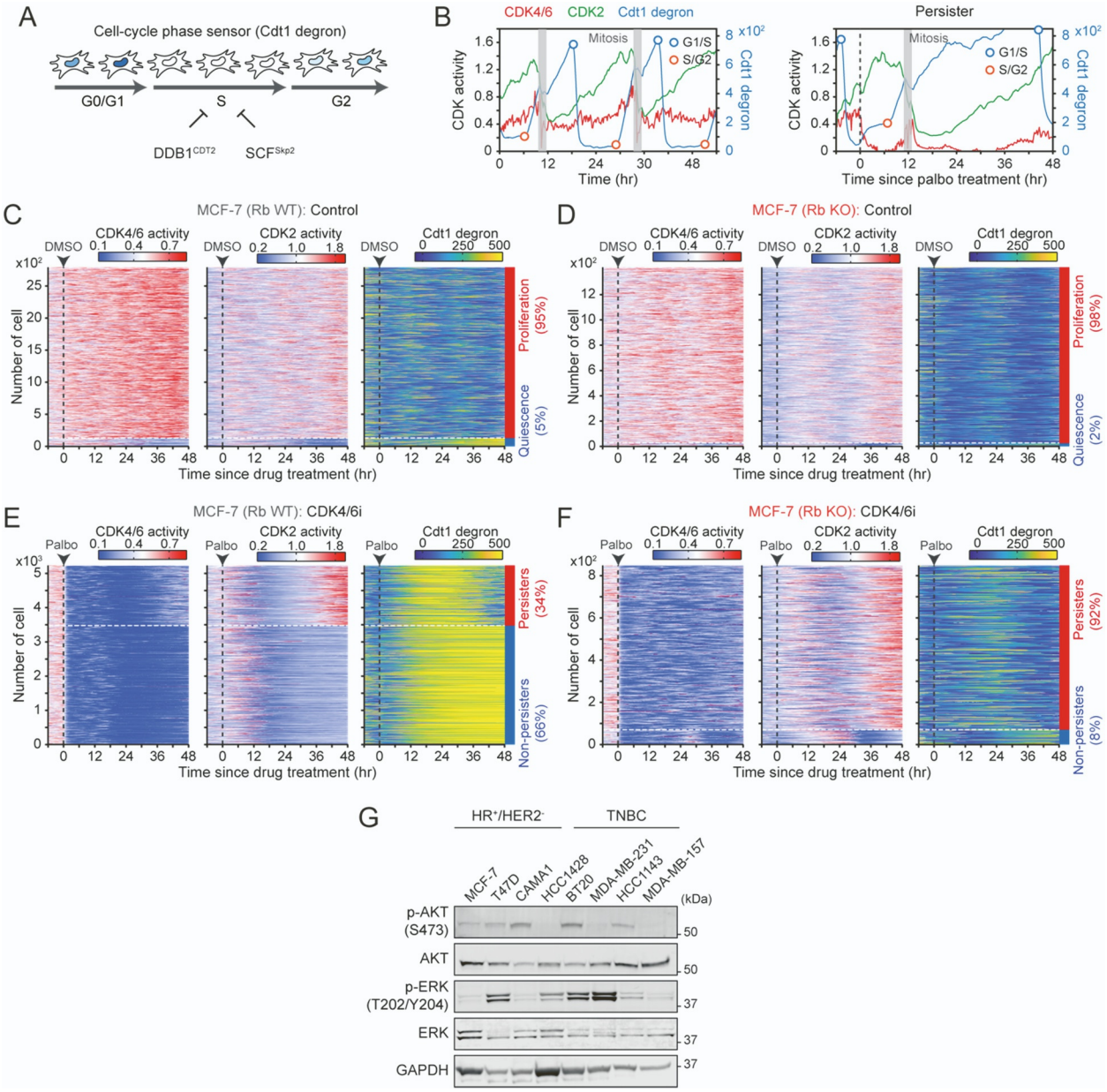

Figure S8. Rb knockout alone is sufficient to induce CDK4/6i adaptation. Related to Figure 6.

(**A**) Schematic diagram depicting the cell cycle phase sensor is based on a Cdt1 degron (a.a 1–100). During S-phase, Cdt1 degron is degraded by two E3 complexes, Cul4-Ddb1^{Cdt2} and Scf^{Skp2}.
(**B**) Single cell traces of CDK4/6 and CDK2 activities and Cdt1 degron intensity in MCF-7 cells. G1/S (blue dot) and S/G2 (orange dot) transitions were labeled. Right: A cell was treated with palbociclib (1μM) and identified as a persister based on CDK2 activity.
(**C**–**F**) Heatmaps of single-cell traces for CDK4/6 and CDK2 activities and Cdt1 degron intensity in wild-type (C, E) and Rb-knockout (D, F) MCF-7 cells treated with either DMSO (C, D) or palbociclib (1 μM) alone (E, F). Each row represents a single-cell trace. The percentages mark the proportion of proliferation or persisters (CDK2 activity >1.0 for more than 2 hr) and quiescence

or non-persisters (no CDK2 activation) cells classified based on CDK2 activity during 30–48 hr after drug treatment. Arrow and black dotted line mark the drug-treatment time.
(**G**) Immunoblot showing expression of p-AKT (S473), AKT, p-ERK (T202/Y204), ERK, and GAPDH in a panel of breast cancer cell lines.

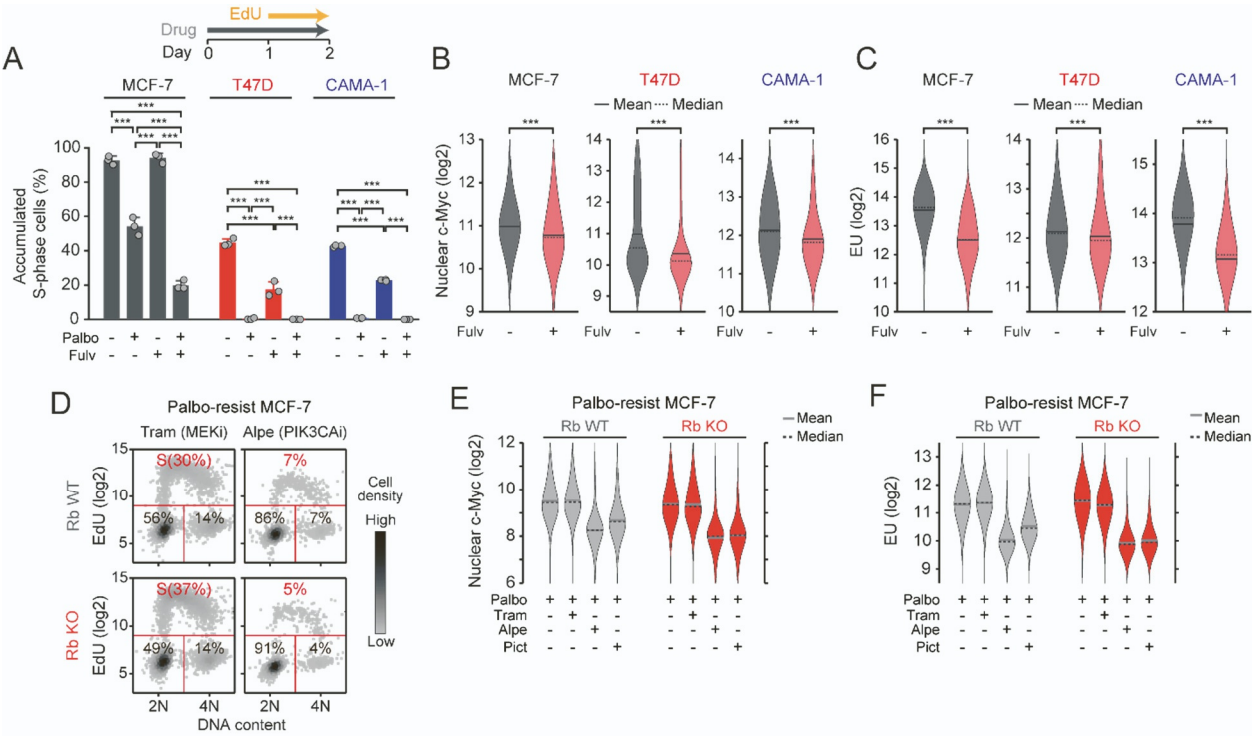

Figure S9. Targeting mitogenic or endocrine signaling inhibits c-Myc, global transcription rate, and CDK4/6i resistance. Related to Figure 6.

(**A**) Percentage of S-phase cells. Cells were treated with DMSO or combinations of palbociclib (1 μM) and fulvestrant (500 nM) for 2 days. Data are shown as means ± SD (n = 3 biological replicates). P values were calculated by one-way ANOVA (*** $p \leq 0.0001$).

(**B** and **C**) Violin plots of c-Myc (B) and EU (C) levels in cells treated with fulvestrant (500 nM) for 2 days. P values were calculated by two-tailed paired t-test (*** $p \leq 0.0001$).

(**D**) Density scatterplot of Hoechst and EdU staining. Wild-type and Rb-knockout MCF-7 cells resistant to palbociclib (1 μM) were treated with trametinib (tram, 100 nM) and alpelisib (alpe, 1 μM) for 2 days (n = 5,000 cells/condition).

(**E** and **F**) Representative violin plots of c-Myc (E) and EU (F) levels in wild-type and Rb-knockout palbociclib-resistant MCF-7 cells treated with DMSO, trametinib (100 nM), alpelisib (1 μM), and pictilisib (250 nM) for 2 days (n = 5,000 cells/condition).

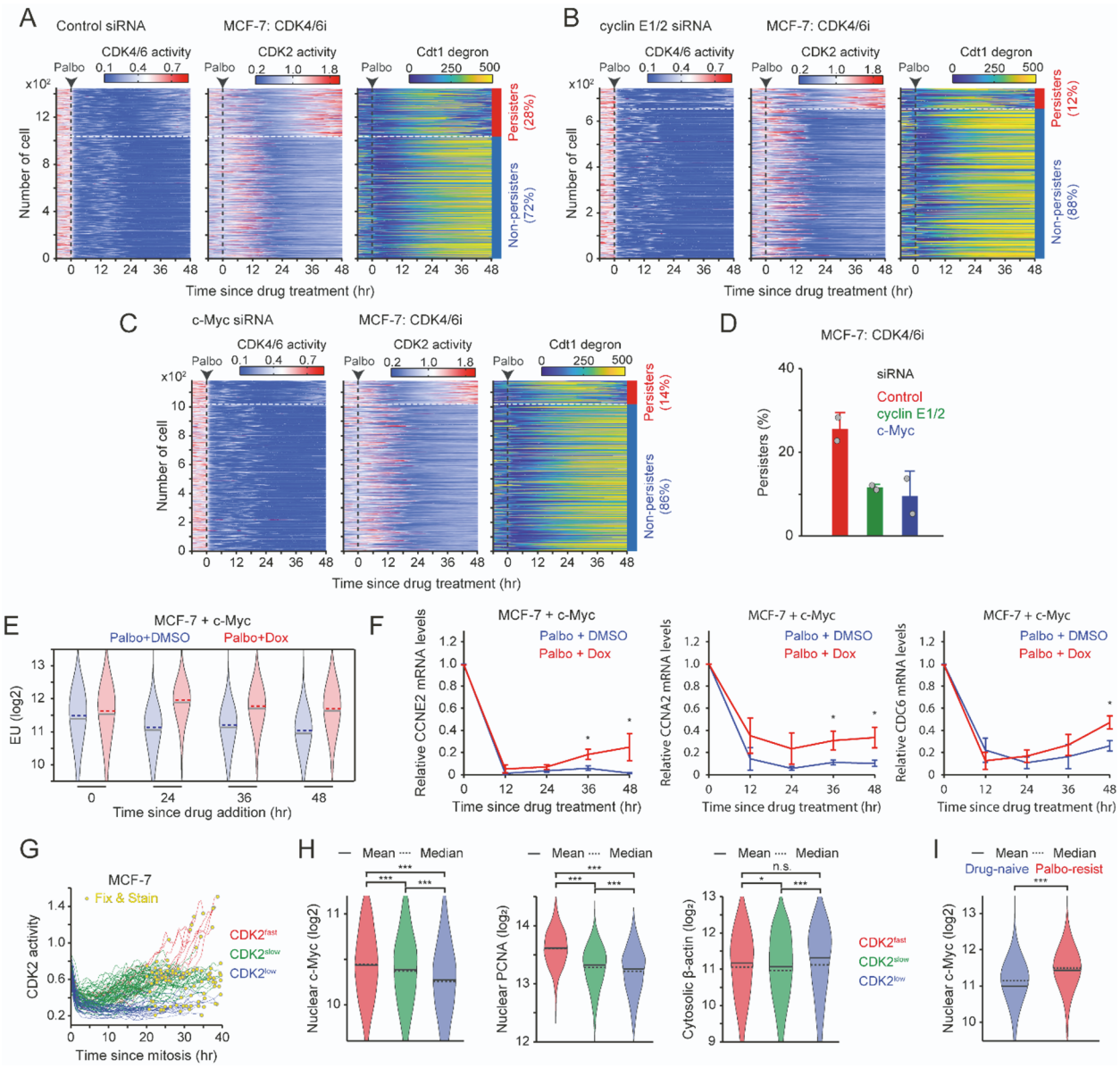

Figure S10. c-Myc amplifies E2F activity to facilitate the development of CDK4/6i-tolerant persisters following Rb-protein reduction. Related to Figure 7.

(**A**–**C**) Heatmaps of single-cell traces for CDK4/6 and CDK2 activities and Cdt1 degron intensity. Each row represents a single-cell trace. MCF-7 cells transfected with control (A), cyclin E1/2 (B), or c-Myc (C) siRNAs 24 hr before live-cell imaging. The percentages mark the proportion of persisters (CDK2 activity >1.0 for more than 2 hr) and non-persisters (no CDK2 activation) cells classified based on CDK2 activity during 30–48 hr after drug treatment. Arrow and black dotted line mark the drug-treatment time.

(**D**) Percentage of persisters after palbociclib (1 μM) treatment in MCF-7 cells transfected with control, cyclin E1/2, or c-Myc siRNA. Data are means ± SD (n = 2 biological replicates).

(**E**) Violin plot represent EU levels at indicated times after treatment with palbociclib (1 μM) plus either DMSO or doxycycline (5 μM) in MCF-7 cells expressing inducible c-Myc (n > 5,000 cells/condition).

(**F**) Relative mRNA expression of E2F target genes, CCNE2, CCNA2, and CDC6, in MCF-7 cells expressing an inducible c-Myc construct. Cells were treated with palbociclib (1 μM) plus either DMSO or doxycycline (5 μM) for indicated time. Data are shown as means ± SD (n = 3 biological replicates). P values were calculated using two-tailed paired t-test (* $p \leq 0.05$).
(**G**) Single-cell traces for CDK2 activity aligned to the time after mitosis. MCF-7 cells were treated with palbociclib (1 μM) and classified based on CDK2 activity 30–48 hr post-treatment: $CDK2^{fast}$ (CDK2 activity >1.0 for over 2 hr), $CDK2^{slow}$ (CDK2 activity >0.6 for over 2 hr), and $CDK2^{low}$ (no CDK2 activation) cells. Yellow points correspond to the time of fixation.
(**H**) Violin plots of c-Myc levels, PCNA, and β-actin in MCF-7 cells classified based on CDK2 activation kinetics after palbociclib (1 μM) treatment (c-Myc: $CDK2^{fast}$, n = 896 cells; $CDK2^{slow}$, n = 5,510 cells; $CDK2^{low}$, n = 2,635 cells; PCNA: $CDK2^{fast}$, n = 1,106 cells; $CDK2^{slow}$, n = 5,634 cells; $CDK2^{low}$, n = 2,592 cells; β-actin: $CDK2^{fast}$, n = 896 cells; $CDK2^{slow}$, n = 5,513 cells; $CDK2^{low}$, n = 2,639 cells). P values were calculated by one-way ANOVA (* $p \leq 0.05$, *** $p \leq 0.0001$).
(**I**) Violin plots of c-Myc levels in drug-naïve and palbociclib-resistant cells (n = 4,000 cells/condition). P values were calculated using two-tailed paired t-test (*** $p \leq 0.0001$).

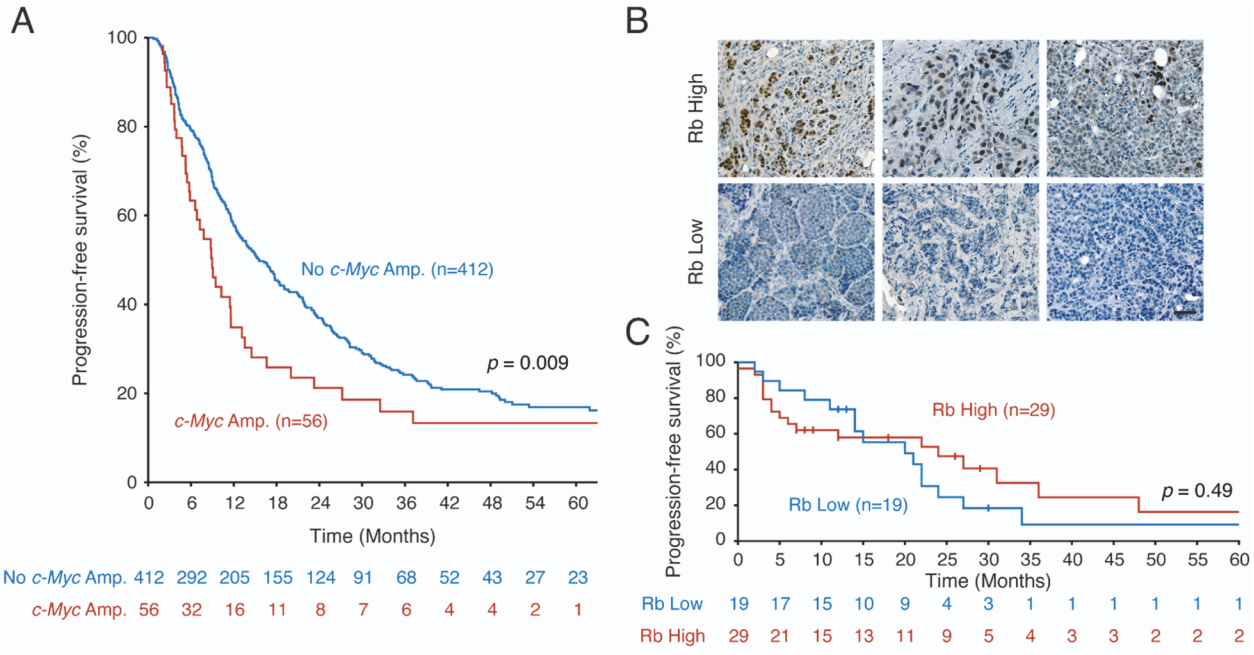

Figure S11. Lack of correlation between Rb levels and PFS in pre-treatment FFPE tumor samples. Related to Figure 7.

(**A**) Kaplan-Meier plots of PFS based on *c-Myc* genetic amplification status, with adjustment for endocrine therapy partner. The *p* value was calculated by the log-rank test.

(**B**) Representative images of pre-treatment tissue samples exhibiting high Rb expression (H-score > 140) or low Rb expression (H-score ≤ 140). Scale bar is 50 μm.

(**C**) Kaplan-Meier plots of PFS in relation to high or low Rb expression levels. The *p* value was calculated by the log-rank testing.

Table S1. Primers for Real-Time PCR. Related to STAR Methods.

Gene	Sequence 5' → 3'
RB1	F: CTCTCGTCAGGCTTGAGTTTG
	R: GACATCTCATCTAGGTCAACTGC
E2F1	F: TCTCGGCCAGGTACTGATG
	R: ACCCTGACCTGCTGCTCTT
MCM2	F: CCGTGACCTTCCACCATTTGA
	R: GGTAGTCCCTTTCCATGCCAT
PCNA	F: CCTGCTGGGATATTAGCTCCA
	R: CAGCGGTAGGTGTCGAAGC
CCNE2	F: TCAAGACGAAGTAGCCGTTTAC
	R: TGACATCCTGGGTAGTTTTCCTC
CCNA2	F: TGGAAAGCAAACAGTAAACAGCC
	R: GGGCATCTTCACGCTCTATTT
RSP23	F: TTCTTGATCAGCTGGACCCT
	R: ACCCTTTTGGAGGTGCTTCT
Ki67	F: ACGCCTGGTTACTATCAAAAGG
	R: CAGACCCATTTACTTGTGTTGGA
CDC6	F: GCCGAACTAGAACAGCATCTT
	R: GGGCTGGTCTAATTTTTCCTGC
mRb1	F: TCGATACCAGTACCAAGGTTGA
	R: ACACGTCCGTTCTAATTTGCTG
mGAPDH	F: AGGTCGGTGTGAACGGATTTG
	R: GGGGTCGTTGATGGCAACA